**Author Response to referee comments on "Coastal ocean acidification and increasing total alkalinity in the NW Mediterranean Sea" by Kapsenberg et al.**

***Overall author response:*** *We thank the Editor for his time and the detailed comments for corrections. For the ease of reviewing our response, we have numbered comments from 1 to 18 and refer to these numbers in the Tracked Changes revised document and in our point-by-point response below in blue.*

---

1. L90 these studies cover various periods … (delete: study ; twice study in this sentence is not necessary). *Deleted "study".*

2. L146-148 "The site Point B is an historical sampling point, since 1957, regarding several oceanographic parameters." Is this sentence ok like this? Looks strange to me. *Revised sentence is: "Point B has been an oceanographic station since 1957".*

3. L150 "predominantly" is definitely more common. *The correction has been made.*

4. L178-182 "Precision of CT and AT was less than 3 µmol kg-1, and the average accuracy was 2.6 and 3 µmol kg-1, as compared with seawater certified reference material (CRM) provided by A. Dickson" To my understanding, the accuracy must always be less good (i.e., higher absolute number) than the precision, because it is superimposed on the precision. *Accuracy was determined as the mean offset between the measured and reference value of the CRMs. Precision refers to the repeatability of attaining the same value across replicate bottle samples (which includes errors associated with sample collection, preservation, etc.). We have updated the text to use the phrase repeatability instead of precision: "Average accuracy of $C_T$ and $A_T$ measurements was 2.6 and 3 µmol $kg^{-1}$, respectively, as compared with seawater certified reference material (CRM) provided by A. Dickson (Scripps Institution of Oceanography). Repeatability of replicate samples was better than 3 µmol $kg^{-1}$."*

5. L276 … that salinity only increased … (suggest to add: only). *Done.*

6. L280 trend (instead of: change)? *Done.*

7. L281 greater (instead of: faster)? *Done.*

8. L351-352 … but still it increased … (add: it)? *Replaced with "but it did increase"*

9. L366 were (not: was) *Done.*

10. L385-391 This part must be moved to the Materials and Methods section. *The information in this section has been moved to the Methods section.*

11. L447-448 … which may result from warming due to increased evaporation) (I think it is useful to add this is not just warming but evaporation following warning) *For simplicity, we have removed the statement indicating that the change in salinity could be associated with warming. This sentence is about trends at 50 m depth. Speculation on the source of salinity change should thus not be attributed to a process that would actually be taking place at the surface. While evaporation could be the source of increasing salinity, one*

*would have to discuss movement of the water mass at 50 m, and hypothesize that when this water mass was at the surface it was subject to evaporation. As we do not have knowledge on water mass movement, we have removed speculation on the change in salinity at 50 m.*

12. L486 … are still in agreement. (not: agreeable) *The sentence has been re-written as: "While the uncertainty for DYFAMED pH data is large, the trends are comparable to those observed at Point B".*

13. L488 I would suggest: This probably indicates that … *Done.*

14. L495 I suggest for clarity: … that may be occurring in more coastal regions of the Mediterranean. *Done.*

15. L496-499 I don't quite understand this. You write about a contrast between the western and eastern Med, but the acidification trends are very similar. *We have removed this sentence.*

16. L516 outgassing (instead of: off-gassing)? *Revised sentence reads "Summer warming leads to $pCO_2$ outgassing".*

17. L589 delete: a. *Done.*

18. Fig. 2g, 3g and 2n, 3n: the symbol on the y-axis is not correct. Also in other figures some symbols were not printed. Please check. *This occurred while converting the Word document to PDF. The high-resolution images do not have this issue.*

# Coastal ocean acidification and increasing total alkalinity in the NW Mediterranean Sea

Lydia Kapsenberg[1], Samir Alliouane[1], Frédéric Gazeau[1], Laure Mousseau[1], and Jean-Pierre Gattuso[1,2,§]

[1]Sorbonne Universités, Université Pierre et Marie Curie-Paris 6, CNRS-INSU, Laboratoire d'Océanographie de Villefranche, 06230, Villefranche-sur-Mer, France

[2]Institute for Sustainable Development and International Relations, Sciences Po, 27 rue Saint Guillaume, F-75007 Paris, France

[§]Corresponding author

E-mail: gattuso@obs-vlfr.fr

Phone: +33 4 93 76 38 59

**Abstract.** Coastal time-series of ocean carbonate chemistry are critical for understanding how global anthropogenic change manifests in near-shore ecosystems. Yet, they are few and have low temporal resolution. At the time-series station Point B in the NW Mediterranean Sea, seawater was sampled weekly from 2007 through 2015, at 1 and 50 m, and analyzed for total dissolved inorganic carbon ($C_T$) and total alkalinity ($A_T$). Parameters of the carbonate system such as pH ($pH_T$, total hydrogen ion scale) were calculated and a deconvolution analysis was performed to identify drivers of change. The rate of surface ocean acidification was -0.0028 ± 0.0003 units $pH_T$ $yr^{-1}$. This rate is larger than previously identified open-ocean trends due rapid warming that occurred over the study period (0.072 ± 0.022 °C $yr^{-1}$). The total $pH_T$ change over the study period was of similar magnitude as the diel $pH_T$ variability at this site. The acidification trend can be attributed to atmospheric carbon dioxide ($CO_2$) forcing (59 %, 2.08 ± 0.01 ppm $CO_2$ $yr^{-1}$) and warming (41 %). Similar trends were observed at 50 m but rates were generally slower. At 1 m depth, the increase in atmospheric $CO_2$ accounted for approximately 40 % of the observed increase in $C_T$ (2.97 ± 0.20 μmol $kg^{-1}$ $yr^{-1}$). The remaining increase in $C_T$ may have been driven by the same unidentified process that caused an increase in $A_T$ (2.08 ± 0.19 μmol $kg^{-1}$ $yr^{-1}$). Based on the analysis of monthly trends, synchronous increases in $C_T$ and $A_T$ were fastest in the spring-summer transition. The driving process of the interannual increase in $A_T$ has a seasonal and shallow component, which may indicate riverine or groundwater influence. This study exemplifies the importance of understanding changes in coastal carbonate chemistry through the lens of biogeochemical cycling at the land-sea interface. This is the first coastal acidification time-series providing multiyear data at high temporal resolution. The data confirm rapid warming in the Mediterranean Sea and demonstrate coastal acidification with a synchronous increase in total alkalinity.

**Keywords –** ocean change, ocean acidification, time-series, pH, alkalinity, dissolved inorganic carbon, $pCO_2$, Mediterranean Sea

## 1. Introduction

Maintaining time-series of oceanographic data is essential for understanding anthropogenic changes in the ocean (Tanhua et al., 2013). On land, fossil fuel burning, cement production, and land use changes have contributed ~600 Gt carbon to the atmosphere during the period 1750-2015 (Le Quéré et al., 2016). In the recent decade 2006-2015, an estimated 25 % of this anthropogenic carbon has been absorbed by the ocean in the form of carbon dioxide ($CO_2$; Le Quéré et al., 2016), and is causing global changes to the ocean carbonate system. Absorption of $CO_2$ by seawater produces carbonic acid, which decreases seawater pH, and is of great concern for biological processes and marine ecosystems (Doney et al., 2009; Gattuso and Hansson, 2011; Pörtner et al., 2014). Since the preindustrial era, global mean ocean pH has declined by 0.1 (Rhein et al., 2013). Due to the declining trend of ocean pH with increasing anthropogenic $CO_2$, the process is termed 'ocean acidification'. This expression represents a suite of chemical changes, including increases in total dissolved inorganic carbon ($C_T$) and partial pressure of $CO_2$ ($pCO_2$) and decrease in calcium carbonate saturation states ($\Omega$, aragonite and calcite; Dickson, 2010). Rates of ocean acidification differ by ocean region and range from -0.0026 (Irminger Sea, North Atlantic) to -0.0013 (South Pacific) units pH $yr^{-1}$ (Bates et al., 2014). Such time-series remain spatially limited, especially in coastal regions, which provide valuable ecosystem services (Barbier et al., 2011; Costanza et al., 1997) and are under high anthropogenic impact (Halpern et al., 2008). Here, we present the first coastal ocean acidification time-series at high temporal resolution.

Compared to the global ocean, marginal seas serve a critical role in anthropogenic $CO_2$ storage via enhanced $CO_2$ uptake and export to the ocean interior (Lee et al., 2011). As a marginal sea, the Mediterranean Sea has a naturally high capacity to absorb but also buffer anthropogenic $CO_2$ (Álvarez et al., 2014; Palmiéri et al., 2015). This is primarily due to the high total alkalinity ($A_T$) of Mediterranean waters and overturning circulation (Lee et al.,

Deleted: ,

Deleted: but t

2011; Palmiéri et al., 2015; Schneider et al., 2010). In the Mediterranean Sea, the salinity-$A_T$ relationship is driven by the addition of river discharge and Black Sea input, which are generally high in $A_T$ (Copin-Montégut, 1993; Schneider et al., 2007). Combined with evaporation, this results in higher $A_T$ and salinity in the Mediterranean Sea compared to the Atlantic Mediterranean source water (Jiang et al., 2014). On average, Mediterranean Sea $A_T$ is 10 % higher than in the global ocean (Palmiéri et al., 2015). The surface ocean acidification rate, estimated at $\Delta pH_T$ (total hydrogen ion scale) of -0.08 since 1800, is comparable to that of the global ocean despite a 10 % greater anthropogenic carbon inventory (Palmiéri et al., 2015). Due to its important role in carbon sequestration and ecological sensitivity to anthropogenic change with economic consequences (Lacoue-Labarthe et al., 2016), the Mediterranean Sea could provide insight to global trends (Lejeusne et al., 2010).

Over the last few years, numerous studies have estimated ocean acidification rates across the Mediterranean Sea (Table 1). Together, these studies cover various periods with a range of techniques yielding different results. For example, estimates of change in pH of bottom waters since the preindustrial era range between -0.005 to -0.06 (Palmiéri et al., 2015) and as much as -0.14 for full profile estimates (Touratier and Goyet, 2011). Techniques for estimating ocean acidification in the Mediterranean Sea thus far include: (1) hind-casting, using high-resolution regional circulation models (Palmiéri et al., 2015), the TrOCA approach as applied to cruise-based profile data (Krasakopoulou et al., 2011; Touratier and Goyet, 2011; Touratier et al., 2016) and others (Howes et al., 2015), (2) partially reconstructed time-series (Marcellin Yao et al., 2016), (3) comparative study periods (Luchetta et al., 2010; Meier et al., 2014), and (4) sensor-based observations over a short study period (Flecha et al., 2015). Ocean acidification time-series of consistent sampling over many years are lacking for the Mediterranean Sea (The MerMex Group et al., 2011),

**Comment [LK1]:** #1

**Deleted:** study

93 particularly along the coast where river discharge influences the carbonate system (Ingrosso
94 et al., 2016).
95 Compared to the open ocean, shallow coastal sites exhibit natural variability in
96 carbonate chemistry over annual timeframes (Hofmann et al., 2011; Kapsenberg and
97 Hofmann, 2016; Kapsenberg et al., 2015), complicating the detection and relevance of open
98 ocean acidification in isolation of other processes (Duarte et al., 2013). In the NW Pacific
99 coast, rapid acidification of surface waters ($\Delta pH_T$ -0.058 units $yr^{-1}$) at Tatoosh Island was
100 documented in the absence of changes in known drivers of local pH variability (e.g.,
101 upwelling, eutrophication, and more; Wootton and Pfister, 2012; Wootton et al., 2008).
102 Further inshore, in the Hood Canal sub-basin of the Puget Sound, only 24-49 % of the
103 estimated pH decline from pre-industrial values could be attributed to anthropogenic $CO_2$
104 (Feely et al., 2010). The excess decrease in pH was attributed to increased remineralization
105 (Feely et al., 2010). Acidification rates documented along the North Sea Dutch coastline and
106 inlets were highly variable in space, with some exceeding the expected anthropogenic $CO_2$
107 rate by an order of magnitude while others exhibited an increase in pH (Provoost et al.,
108 2010).
109 Variability in coastal carbonate chemistry stems from both physical (e.g., upwelling,
110 river discharge; Feely et al., 2008; Vargas et al., 2016) and biological processes (e.g., primary
111 production, respiration, net calcification). Within watersheds, coastal carbonate chemistry is
112 affected by eutrophication (Borges and Gypens, 2010; Cai et al., 2011), groundwater supply
113 (Cai et al., 2003), and land use and rain influence on river alkalinity (Raymond and Cole,
114 2003; Stets et al., 2014). Over longer periods, pH can also be influenced by atmospheric
115 deposition (Omstedt et al., 2015). Through primary production and respiration, coastal
116 ecosystems produce pH fluctuations over hours (e.g., seagrass, kelp) to months (e.g.,
117 phytoplankton blooms; Kapsenberg and Hofmann, 2016). Due to existing pH variability in

coastal seas, it is necessary to quantify high-frequency trends in order to interpret the pH changes inferred from lower-frequency sampling.

In this study, we present the first complete time-series data quantifying the present-day ocean acidification rate for a coastal site in the Mediterranean Sea, based on weekly measurements of $A_T$ and $C_T$ sampled from 2007 through 2015. For a subset of this time-series, pH variability was documented using a SeaFET™ Ocean pH Sensor in order to assess hourly pH variability. For comparison and consistency with other ocean acidification time-series around the world, we report rates of change based on anomalies (Bates et al., 2014) and identify drivers of change.

## 2. Materials and methods

### 2.1. Site description

A carbonate chemistry time-series was initiated in 2007 and maintained through 2015 in the NW Mediterranean Sea at the entrance of the Bay of Villefranche-sur-Mer, France (Fig. 1): Point B station (43.686° N, 7.316° E, 85 m bottom depth). A second site, Environment Observable Littoral buoy (EOL, 43.682° N, 7.319° E, 80 m bottom depth), was used for pH sensor deployment starting in 2014. These two sites are 435 m apart. Point B has been an oceanographic station since 1957. A full site description and research history has been detailed by De Carlo et al. (2013). Briefly, the Bay is a narrow north-south facing inlet with steep bathymetry and estimated volume of 310 million $m^3$. The surrounding region is predominantly composed of limestone with a series of shallow, submarine groundwater karst springs (Gilli, 1995). The North current, a major and structuring counter-clockwise current in the Ligurian Sea, can sometimes flow close to Point B. The Bay can also be, on occasion, influenced by local countercurrents. Both of these hydrodynamics movements have

**Comment [LK2]:** #2
**Deleted:** The site
**Deleted:** is an historical
**Deleted:** sampling point
**Deleted:** ,
**Deleted:** , regarding several oceanographic parameters

**Comment [LK3]:** #3
**Deleted:** e

149 signatures of river discharge. Limestone erosion can be observed in the $A_T$ of rivers nearest to
150 Point B (Paillon, due 4 km West; Var due 10 km West; and Roya due 26 km East). River $A_T$
151 ranges between 1000 to 2000 µmol kg$^{-1}$ (data from *Agence de l'Eau Rhône-Méditerranée-*
152 *Corse*, http://sierm.eaurmc.fr), and is lower than seawater $A_T$. The Paillon River, whose
153 plume on occasion reaches into the Bay (L. Mousseau, pers. obs.), was sampled on 18 August
154 2014 and had a $A_T$ of 1585 ± 0.1 µmol kg$^{-1}$ ($N$ = 2, J.-P. Gattuso, unpubl.). Due to low
155 primary productivity, seasonal warming drives the main annual variability in carbonate
156 chemistry at this location (De Carlo et al., 2013).
157
158 **2.2. Point B data collection, processing, and analysis**
159 To document long-term changes in ocean carbonate chemistry at Point B, seawater
160 was sampled weekly from 9 January 2007 to 22 December 2015. Samples were collected at 1
161 and 50 m, using a 12-L Niskin bottle at 9:00 local time. Seawater was transferred from the
162 Niskin bottle to 500 mL borosilicate glass bottles and fixed within an hour via addition of
163 saturated mercuric chloride for preservation of carbonate parameters, following
164 recommendations by Dickson et al. (2007). Duplicate samples were collected for each depth.
165 For each sampling event, CTD casts were performed either with a Seabird 25 or Seabird 25+
166 profiler whose sensors are calibrated at least every two years. Accuracy of conductivity
167 (SBE4 sensor) and temperature (SBE3 sensor) measurements from CTD casts were 0.0003 S
168 m$^{-1}$ and 0.001°C, respectively.
169 Within six months of collection, bottle samples were analyzed for $C_T$ and $A_T$ via
170 potentiometric titration following methods described by Edmond (1970) and DOE (1994), by
171 *Service National d'Analyse des Paramètres Océaniques du $CO_2$*, at the Université Pierre et
172 Marie Curie in Paris, France. Average accuracy of $C_T$ and $A_T$ measurements was 2.6 and 3
173 µmol kg$^{-1}$, respectively, as compared with seawater certified reference material (CRM)

**Comment [LK5]:** #4
**Deleted:** Precision of $C_T$ and $A_T$
**Deleted:** was less than 3 µmol kg$^{-1}$, and the average
**Deleted:** a

provided by A. Dickson (Scripps Institution of Oceanography). Repeatability of replicate samples was better than 3 µmol $kg^{-1}$. Only obvious outliers were omitted from the analyses: three $C_T$ values at 1 m (> 2300 µmol $kg^{-1}$), one $A_T$ value at 1 m (> 2900 µmol $kg^{-1}$), and one $A_T$ value at 50 m (< 2500 µmol $kg^{-1}$). The $C_T$ and $A_T$ measurements on replicate bottle samples were averaged for analyses.

Calculations of the carbonate system parameters were performed using the R package seacarb version 3.1 with $C_T$, $A_T$, *in situ* temperature, and salinity as inputs (Gattuso et al., 2016). Total concentrations of silicate ($SiOH_4$) and phosphate ($PO_4^{3-}$) were used when available from Point B (L. Mousseau, unpubl., http://somlit.epoc.u-bordeaux1.fr/fr/). Detection limits for nutrients were 0.03 µM for $SiOH_4$ and 0.003 to 0.02 µM for $PO_4^{3-}$; relative precision of these analyses is 5-10 % (Aminot and Kérouel, 2007). Total boron concentration was calculated from salinity using the global ratio determined by Lee et al. (2010). The following constants were used: $K_1$ and $K_2$ from Lueker et al. (2000), $K_f$ from Perez and Fraga (1987), and $K_s$ from Dickson (1990). Reported measured parameters are temperature, salinity, $A_T$, and $C_T$, and derived parameters are $pH_T$ (total hydrogen ion scale), $pH_T$ normalized to 25 ºC ($pH_{T25}$), $pCO_2$, and aragonite ($\Omega_a$) and calcite ($\Omega_c$) saturation states. Salinity-normalized changes in $A_T$ ($nA_T$) and $C_T$ ($nC_T$) were calculated by dividing by *in situ* salinity and multiplying by 38. Except for $pH_{T25}$, all parameters are reported at *in situ* temperatures.

The average uncertainties of the derived carbonate parameters were calculated according to the Gaussian method (Dickson and Riley, 1978) implemented in the "errors" function of the R package seacarb 3.1 (Gattuso et al., 2016). The uncertainties are ± 2.7 x $10^{-10}$ mol $H^+$ (about 0.015 units $pH_T$), ± 15 µatm $pCO_2$, and ± 0.1 unit of the aragonite and calcite saturation states.

To quantify interannual changes in carbonate parameters, the data were detrended for seasonality by subtracting the respective climatological monthly means computed for the period 2009-2015 from the time-series ('monthly means' from hereon). The resulting residuals were analyzed using a linear regression to compute anomaly trends. This approach follows methods from Bates et al. (2014) to allow for comparisons of trends observed at different time-series stations. All analyses were performed in R (R Core Team, 2016).

### 2.3. Deconvolution of $pH_T$ and $pCO_2$

To identify proportional contributions of various drivers to ocean acidification trends at Point B, deconvolution of time-series $pH_T$ and $pCO_2$ was performed following methods from García-Ibáñez et al. (2016) for observations at 1 and 50 m. The equation is described below for $pH_T$, where changes in $pH_T$ are driven by changes in temperature ($T$), salinity ($S$), $A_T$, and $C_T$, over time ($t$):

Deleted: , according to the following model

$$\frac{dpH_T}{dt} = \frac{\partial pH_T}{\partial T}\frac{dT}{dt} + \frac{\partial pH_T}{\partial S}\frac{dS}{dt} + \frac{\partial pH_T}{\partial A_T}\frac{dA_T}{dt} + \frac{\partial pH_T}{\partial C_T}\frac{dC_T}{dt} \quad (1)$$

Here, $\frac{\partial pH_T}{\partial var}\frac{dvar}{dt}$ represents the slope contribution of changing *var* to the estimated change in $pH_T$ ($\frac{dpH_T}{dt}$), where *var* is either temperature (T), salinity (S), $A_T$, or $C_T$. The sensitivity of pH to *var* ($\frac{\partial pH_T}{\partial var}$) was estimated by calculating $pH_T$ using the true observations of *var* and holding the other three variables constant (mean value of the time-series) and regressing it to *var*. Sensitivity ($\frac{\partial pH_T}{\partial var}$) was then multiplied by the anomaly rate of *var* (Table 2). The calculation was repeated for $pCO_2$ ($\frac{dpCO_2}{dt}$) in order to compare the rate of increase with that of atmospheric $CO_2$.

As a sub-component of $\frac{\partial pCO_2}{\partial C_T}\frac{dC_T}{dt}$, the rate of anthropogenic $CO_2$ increase was estimated from atmospheric $CO_2$ concentrations nearest to Point B (Plateau Rosa, Italy,

courtesy of the World Data Center for Greenhouse Gases, http://ds.data.jma.go.jp/gmd/wdcgg/). For these data, missing daily values were linearly interpolated, climatological monthly means were calculated and subtracted from the time-series to generate an anomaly time-series. A linear regression was performed on anomalies where the slope represents the rate of anthropogenic $CO_2$ increase in the atmosphere. Finally, to help identify different processes that might have contributed to the observed trends, linear regressions were performed on changes in $A_T$ and $C_T$ per month (mean value of observations within one month) from 2009 through 2015 and on the salinity-$A_T$ relationship by year.

**2.4. SeaFET data collection, processing, and analysis**

To capture pH variability at higher-than-weekly sampling frequencies, a SeaFET™ Ocean pH sensor (Satlantic) was deployed on the EOL buoy (435 m from the Point B sampling site) starting in June 2014, at 2 m depth. Autonomous sampling was hourly and deployment periods averaged 58 ± 25 days with 5 ± 2 calibration samples per deployment.

Field calibration samples for pH were collected using a Niskin bottle next to SeaFET within 15 min of measurement. This sampling scheme was sufficient for this site as there is no large high-frequency pH variability. Unlike Point B sampling, SeaFET calibration samples were processed for pH using the spectrophotometric method (Dickson et al., 2007) with purified m-cresol purple (purchased from the Byrne lab, University of South Florida). *In situ* temperature, salinity, and $A_T$ measured at Point B, within 30 min of the SeaFET sampling, were used to calculate *in situ* $pH_T$ of the calibration samples.

SeaFET voltage was converted to $pH_T$ using the respective calibration samples for each deployment period, following the methods and code described in Bresnahan et al. (2014) but adapted for use in R. Only 5 % of the data was removed during quality control, due to biofouling in one deployment and battery exhaustion in another, yielding 610 days of

**Comment [LK6]:** #10

**Deleted:** ranged between 1 and 3 months. Deployment periods

**Moved (insertion) [1]**

**Deleted:** weekly,

**Comment [LK7]:** #10

data. The mean offset between calibration samples and the calibrated SeaFET pH time-series was ± 0.007, indicating a high-quality pH dataset (data shown in Fig. 7c).

The estimated standard uncertainty in SeaFET $pH_T$ is ± 0.01 and was calculated as the square root of the sum of each error squared. The sources of errors are: measurement error of spectrophotometric pH (± 0.004, $N$ = 68 mean SD of 5 replicate measurements per calibration sample for samples collected between 16 July 2014 and 3 May 2016), spatio-temporal mismatch sampling at EOL (± 0.007, mean offset of $pH_T$ of the calibration samples from calibrated time-series), and variability in purified m-cresol dye batch accuracy as compared to Tris buffer CRM pH (± 0.006, mean offset of $pH_T$ of the spectrophotometric measurement of Tris buffer from the CRM value).

## 3. Results

### 3.1. Time-series trends

At Point B from January 2007 to December 2015, more than 400 samples were collected for carbonate chemistry at both 1 and 50 m. Anomaly trends detected at 1 m (Fig. 2) were also significant at 50 m (Fig. 3, Table 2), with the exception that salinity only increased at 50 m (0.0063 ± 0.0020 units $yr^{-1}$). At 1 m, trends were significant for $pH_T$ (-0.0028 units $yr^{-1}$), $A_T$ (2.08 µmol $kg^{-1}$ $yr^{-1}$), $C_T$ (2.97 µmol $kg^{-1}$ $yr^{-1}$), $pCO_2$ (3.53 µatm $yr^{-1}$), and $\Omega_a$ (-0.0064 units $yr^{-1}$). At the same time, temperature anomaly increased (0.072 ºC $yr^{-1}$). Changes in carbonate chemistry parameters were greater at 1 m compared to 50 m, with the exception of salinity and temperature. The warming rate at 50 m was slightly greater compared to 1 m, mostly due to increasing summer temperatures since 2007.

Strong seasonal cycles of carbonate chemistry parameters were present at Point B at 1 m (Fig. 4). Climatological monthly means (2007-2015) are described briefly and listed in

**Comment [LK8]:** #5

**Deleted:** , but no significant change in the salinity was detected at 1 m

**Deleted:** Trends

**Comment [LK9]:** #6

**Comment [LK10]:** #7

**Deleted:** o

**Deleted:** f

**Deleted:** faster

Table S1. Mean temperature range was 11.2 ºC with a maximum at 24.77 ± 1.35 ºC in August and minimum of 13.58 ± 0.41 ºC in February. The range in $A_T$ was 19 µmol kg$^{-1}$ from June to September. The $C_T$ range was 33 µmol kg$^{-1}$ with a peak in late winter and minimum values in August and October. Due to summer warming coinciding with the period of peak primary productivity (De Carlo et al. 2013), warming countered the influence of low $C_T$ on pH. As a result, $pH_T$ reached minimum values in summer (8.02 ± 0.03, July and August) and peaked in late winter (8.14 ± 0.01, February and March), for an overall annual pH range of 0.12. The corresponding $pCO_2$ range was 128 µatm from February to August. Seasonal cycles were smaller at 50 m compared to 1 m (Table S1).

### 3.2. Deconvolution of $pH_T$ and $pCO_2$

Deconvolutions of pH and $pCO_2$ are presented in Table 3 and 4, respectively. The estimated anomaly trends ($\frac{dpH_T}{dt}$ ,$\frac{dpCO_2}{dt}$) from the deconvolution fall within the error of the observed anomaly trends (Table 2). The contribution of warming to the $pH_T$ anomaly (-0.0011 units yr$^{-1}$, at 1 m) matched the difference between the trends of $pH_T$ and $pH_{T25C}$ (Table 2), which verifies that the deconvolution reproduced influences of temperature sensitivity well. Overall, these results indicate that the deconvolution analyses represent the observed trends well.

At both depths, the predominant driver of $\frac{dpH_T}{dt}$ and $\frac{dpCO_2}{dt}$ was the increase in $C_T$. Increasing $A_T$ countered 66-69 and 60 % of the influence of increasing $C_T$ on $\frac{dpH_T}{dt}$ and $\frac{dpCO_2}{dt}$, respectively. At 1 m, warming accounted for 41 and 37 % of $\frac{dpH_T}{dt}$ and $\frac{dpCO_2}{dt}$, respectively. Since warming was slightly greater at 50 m compared to 1 m, warming accounted for a larger proportional influence on $\frac{dpH_T}{dt}$ and $\frac{dpCO_2}{dt}$ at 50 m compared to 1 m. Increasing salinity at 50 m contributed slightly to $\frac{dpH_T}{dt}$ (4 %) and $\frac{dpCO_2}{dt}$ (2 %).

Atmospheric $CO_2$ anomaly at Plateau Rosa increased by 2.08 ± 0.01 ppm $yr^{-1}$ ($F_{1,3285}$ = 4664, $P$ <<0.001, $R^2$ 0.93) during the study period 2007-2015, and represents the anthropogenic $CO_2$ forcing on seawater pH. To estimate the influence of anthropogenic $CO_2$ forcing at Point B, we assume air-sea $CO_2$ equilibrium (e.g., increase in atmospheric $CO_2$ causes an equal increase in seawater $pCO_2$) for the water mass at 1 m. This assumption is based on evidence that Point B is a weak sink for atmospheric $CO_2$ with near-balanced air-sea $CO_2$ flux on an annual time-frame (De Carlo et al., 2013). Considering the error associated with deconvolution of $pCO_2$ at 1 m, atmospheric $CO_2$ increase can, at most, represent 38-43 % of the total $C_T$ contribution ($\frac{\partial pCO_2}{\partial C_T}\frac{dC_T}{dt}$) to $\frac{dpCO_2}{dt}$. This leaves 57-62 % of the total $C_T$ contribution to $pCO_2$ trends unaccounted for.

As $A_T$ is not influenced by addition of anthropogenic $CO_2$ to seawater, but it did increase, the next question was whether or not the changes in $A_T$ and $C_T$ were process-linked. At 1 m, regressions of annual monthly trends of $A_T$ and $C_T$ revealed similar seasonal cycles for both parameters (Fig. 5, Table S2). The fastest increases in $A_T$ and $C_T$ occurred from May through July. The smallest (non-significant) changes occurred in January. The synchronicity between monthly trends of $A_T$ and $C_T$ was also observed at 50 m, but the rates were slower (analysis not shown).

Deleted: still

Comment [LK11]: #8

Deleted: d

### 3.3. Salinity and $A_T$ relationships

Over an annual observation period at 1 m, salinity was a poor predictor of $A_T$, with the exception of 2007 (Fig. 6). The $R^2$ value for each annual salinity-$A_T$ relationship at 1 m ranged from 0.00 (in 2013) to 0.87 (in 2007) with y-intercepts ($A_{T0}$, total alkalinity of the freshwater end-member) ranging between -176 µmol $kg^{-1}$ (in 2007) and 2586 µmol $kg^{-1}$ (in 2013). The interannual variability of the salinity-$A_T$ relationship was driven by the variability in $A_T$ observed at salinity < 38.0 that was present from November through July.

Changes in salinity (based on monthly means) at Point B were small and ranged from 37.64 ± 0.26 to 38.21 ± 0.11 from May to September, following freshwater input in winter and spring and evaporation throughout summer and fall (Fig. 4). Highest (> 38.0) and most stable salinity observations were made in August through October and coincided with the period of maximum $A_T$ (2562 and 2561 ± 9 µmol kg$^{-1}$ in September and October, respectively). Minimum $A_T$ (2543 ± 14 µmol kg$^{-1}$) was observed in June, one month after minimum salinity. To capture this seasonality without the inter-annual variation of $A_T$, the salinity-$A_T$ relationship at 1 m was estimated from climatological monthly means ($cA_T$ and *cS, N=12*) where $cA_T$ units are µmol kg$^{-1}$ and error terms are standard errors ($R^2$ = 0.74):

$$cA_T = 1554.9(\pm 185.9) + 26.3(\pm 4.9) \times cS \qquad (2)$$

At 50 m, monthly salinity and $A_T$ were less correlated over an annual cycle (analysis not shown). Salinity remained stable at 38.0 from January through September while $A_T$ declined by 13 µmol kg$^{-1}$. In general, seasonal changes were dampened at 50 m compared to 1 m.

### 3.4. High-frequency pH data

To verify the weekly sampling scheme at Point B, a continuous record of high-frequency pH observations was obtained via SeaFET deployments from June 2014 to April 2016 (Fig. 7). Sensor data corroborated the seasonal pH and temperature cycle observed at Point B (Fig. 7a-b). Event-scale effects (e.g., $pH_T$ change ≥ 0.1 for days to weeks, *sensu* Kapsenberg and Hofmann 2016) were absent at this site suggesting that weekly sampling was sufficient to describe seasonal and interannual changes in carbonate chemistry at Point B. The magnitude of diel $pH_T$ variability was small; the 2.5$^{th}$ to 97.5$^{th}$ percentiles ranged between 0.01 and 0.05 units $pH_T$ (Fig. 7d-e). Variability increased from winter to spring with the greatest variations in April, May, and June ($\Delta pH_T$ >0.035). The magnitude of diel pH

**Comment [LK12]:** #9
**Deleted:** as
**Comment [LK13]:** #10
**Deleted:** 11 consecutive
**Moved up [1]:** Deployment periods averaged 58 ± 25 days with 5 ± 2 calibration samples per deployment (Fig. 7). Only 5 % of the data was removed during quality control, due to biofouling in one deployment and battery exhaustion in another, yielding 610 days of data. The mean offset between calibration samples and the calibrated SeaFET pH time-series was ± 0.007, indicating a high-quality pH dataset (Fig. 7c).
**Deleted:** (
**Deleted:** ,
**Deleted:** Diel pH v
**Deleted:** tions
**Deleted:** bility

variability was not correlated with temperature or the concentration of chlorophyll-a (data not shown).

## 4. Discussion

High resolution time-series are necessary to document coastal ocean acidification. Based on weekly measurements from 2007 through 2015, near-surface $pH_T$ decreased by $0.0028 \pm 0.0003$ units $yr^{-1}$ at Point B in the NW coastal Mediterranean Sea. Temperature increased by $0.072 \pm 0.022$ °C $yr^{-1}$. In addition, $A_T$ increased by $2.08 \pm 0.19$ µmol $kg^{-1}$ $yr^{-1}$, a change that is unrelated to direct effects of $CO_2$ absorption by seawater. In less than a decade, the total change in pH at Point B ($\Delta pH_T$: 0.0252, Table 1) was of the same magnitude as the diel pH variability ($\Delta pH_T$: 0.01-0.05) and $1/5^{th}$ of the magnitude of the seasonal pH cycle ($\Delta pH_T$: 0.12) found at this site.

We can identify the drivers of ocean acidification at Point B using the deconvolution of pH and $pCO_2$ trends and by assuming that the increase in $A_T$ was due to increases in its carbon constituents, bicarbonate ($HCO_3^-$) and carbonate ($CO_3^{2-}$) ions. This assumption is based on the fact that (1) $HCO_3^-$ and $CO_3^{2-}$ ions together make up 96 % of $A_T$ at Point B, (2) increases in $HCO_3^-$ and $CO_3^{2-}$ would both contribute to $A_T$ and $C_T$ and thereby explain the observed synchronicity of monthly trends in $A_T$ and $C_T$ (Fig. 5). Using the $pCO_2$ deconvolution, we can then sum the contributions to $pCO_2$ from $A_T$ (-3.08 µatm $pCO_2$ $yr^{-1}$) and $C_T$ (5.14 µatm $pCO_2$ $yr^{-1}$) to determine the proportional contribution of $\Delta C_T$ to $\Delta pCO_2$ that is unrelated to changes in $C_T$ brought on by $A_T$. This remaining 2.06 µatm $pCO_2$ $yr^{-1}$ increase due to increasing $C_T$ closely matched the magnitude of atmospheric $CO_2$ increase during the observation period ($2.08 \pm 0.01$ ppm $yr^{-1}$ at Plateau Rosa, Italy). The closeness of these numbers does not imply causation. However, given that surface waters at Point B exhibit a near-zero air-sea $CO_2$ flux over annual cycles (De Carlo et al., 2013), the evidence

Deleted: At Point B in the NW coastal Mediterranean Sea,

Deleted: , based on weekly measurements from 2007 through 2015

Deleted: for the

Deleted: trends

Deleted: trends

supports the conclusion that the ocean acidification trend at Point B closely follows the rate of atmospheric $CO_2$ increase. The influence of atmospheric $CO_2$ can also be observed in the monthly changes in $C_T$. Monthly $C_T$ trends are positive and statistically significant over more months than $A_T$ trends (8 vs. 3 months), which are more seasonally restricted (Fig. 5).

Applying this simple model to $pH_T$, assuming changes in $C_T$ are due to both increasing $A_T$ (a neutralizing effect) and atmospheric $CO_2$ forcing, the surface ocean acidification trend at Point B can be attributed primarily to atmospheric $CO_2$ forcing (59 %) and secondarily to warming (41 %).

Using this same approach for observations at 50 m, the $C_T$ contribution to $pCO_2$ trends that was unrelated to $A_T$ change was 1.41 µatm $pCO_2$ $yr^{-1}$, which is 68 % of the rate of atmospheric $CO_2$ increase in contrast to 99 % at 1 m. Changes in $pH_T$ can then be attributed to atmospheric $CO_2$ forcing (42 %), warming (54 %), and increasing salinity (3 %). Due to slightly enhanced warming and reduced $CO_2$ penetration observed at 50 m, warming had a greater effect on the ocean acidification trend than atmospheric $CO_2$ forcing at depth compared to the surface.

**Comment [LK14]:** #11

**Deleted:** , which may result from warming

The acidification rate at Point B (-0.0028 units $pH_T$ $yr^{-1}$) is larger than those reported for other ocean time-series sites (-0.0026 to -0.0013 units pH $yr^{-1}$, Bates et al., 2014), likely due to differences in warming rates. The observed warming from 2007 through 2015 (0.72 to 0.88 ± 0.2 °C $decade^{-1}$) is extremely rapid relative to global trends in the upper 75 m from 1971 to 2010 (0.11 °C $decade^{-1}$, Rhein et al., 2013). The coastal region of Point B has warmed steadily since 1980 and with periods of rapid warming (Parravicini et al., 2015). Exacerbated warming may be related to the positive phases of the Atlantic Multi-decadal Oscillation (AMO) and North Atlantic Oscillation (NAO), both of which are associated with episodic warming of the Mediterranean Sea (Lejeusne et al., 2010). The AMO has been

positive since the 1990s[1] and positive NAO phases were prevalent during the second half of our study[2].

Nearest to Point B, the acidification rate at DYFAMED, an open-sea site about 50 km offshore from Point B (Fig. 1), was estimated at -0.003 ± 0.001 units $pH_{SW}$ $yr^{-1}$ from 1995 to 2011 (Marcellin Yao et al., 2016). At DYFAMED, warming contributed approximately 30 % to the acidification rate and the remaining 70 % was attributed to anthropogenic $CO_2$ (Marcellin Yao et al., 2016). While the uncertainty for DYFAMED pH data is large, the trends are comparable to those observed at Point B. However, $A_T$ at the DYFAMED did not change significantly from 2007 through 2014 ($F_{1,51}$ 3.204, $P$ = 0.0794, $R^2$ 0.08, data from Coppola et al., 2016). This probably indicates that the processes driving changes in $A_T$ at Point B are unique to the coastal environment.

Similar changes in coastal carbonate chemistry were observed elsewhere in the near-shore Mediterranean Sea. In the Northern Adriatic Sea, Luchetta et al. (2010) determined an acidification rate of -0.0025 units $pH_T$ $yr^{-1}$ and an increase in $A_T$ of 2.98 µmol $kg^{-1}$ $yr^{-1}$ at depths shallower than 75 m, by comparing cruise data between the winters of 1983 and 2008. Point B and Adriatic Sea observations are independent but reflect changes in seawater chemistry that may be occurring in more coastal regions of the Mediterranean. Additional time-series would help resolve the spatial extent of these observations.

While the trends in atmospheric $CO_2$ forcing and temperature account for the ocean acidification trend at Point B, the increase in $A_T$ and $C_T$ beyond what can be attributed to changes in atmospheric $CO_2$ was unexpected. The fastest increases in $A_T$ and $C_T$ occurred from May through July (Fig. 5), when the thermal stratification settles. In the NW Mediterranean, the main processes governing seasonal variability in $A_T$ are evaporation

[1] http://www.cgd.ucar.edu/cas/catalog/climind/AMO.html
[2] http://www.cpc.ncep.noaa.gov/products/precip/CWlink/pna/month_nao_index.shtml



**Comment [LK15]:** #12
**Deleted:** The
**Deleted:** and makes direct comparison with Point B unreliable but
**Deleted:** results
**Deleted:** agreeable
**Comment [LK16]:** #13
**Deleted:** may
**Deleted:** in $pH_T$
**Deleted:** across a wider
**Comment [LK17]:** #15
**Deleted:** ed trend
**Deleted:** Specifically, the Eastern Mediterranean Sea would offer an important contrast, as pH of eastern waters is expected to be more sensitive to atmospheric $CO_2$ addition due to their ability to absorb more anthropogenic $CO_2$ than either the western Mediterranean or Atlantic waters (Álvarez et al., 2014).
**Deleted:** increase

469 increasing $A_T$ in summer (i.e., June through September at Point B) and, to a lesser extent,
470 phytoplankton uptake of nitrate ($NO_3^-$) and phosphate ($PO_4^{3-}$) increasing $A_T$ from January
471 through March (Cossarini et al., 2015). During the transition of these processes, salinity
472 decreases to a minimum in May, reflecting freshwater input that dilutes $A_T$ to minimum
473 values at the start of summer. For $C_T$, peak values occur in winter when the water column is
474 fully mixed. For reference, at DYFAMED, mixing occurs down to more than 2000 m depth
475 and $C_T$ is up to 100 µmol $kg^{-1}$ higher in deep waters (Copin-Montégut and Bégovic, 2002).
476 Notably, monthly trends of $C_T$ at Point B were not statistically significant from November
477 through January for the period 2007-2015. Following winter, $C_T$ declines due to a
478 combination of phytoplankton bloom carbon uptake and freshwater dilution (assuming river
479 $C_T$ < seawater $C_T$), until the onset of summer stratification. Summer warming leads to $pCO_2$
480 outgassing (De Carlo et al., 2013), thereby further decreasing $C_T$. In addition, the increases in
481 $A_T$ and $C_T$ from 2007 through 2015 were more pronounced at 1 m compared to 50 m. Thus,
482 the process driving $A_T$ and $C_T$ trends are stronger at the surface and affect carbonate
483 chemistry primarily during the spring-summer transition from May through July.
484 Identifying the process causing an increase in $A_T$ and $C_T$ beyond what can be
485 attributed to changes in atmospheric $CO_2$ requires some speculation. Some biogeochemical
486 processes can be ruled out as drivers. For example, changes in benthic processes are very
487 unlikely. Reduced calcium carbonate ($CaCO_3$) precipitation rates would increase $A_T$ but
488 would increase $C_T$. Even so, the dominant ecosystem in the Bay of Villefranche-sur-Mer is
489 seagrass meadows, which harbor relatively few calcifying organisms. Dissolution of calcium
490 carbonate sediment would contribute to $A_T$ and $C_T$ increase in the water column. However, as
491 the water was supersaturated with respect to both aragonite and calcite, this could only be
492 mediated by biological processes. Carbonate dissolution following $CO_2$ production via oxic
493 degradation of organic matter releases $A_T$ and $C_T$ in a 1:1 ratio (Moulin et al., 1985).

**Comment [LK18]:** #16
**Deleted:** off-
**Deleted:** to the atmosphere
**Deleted:** T
**Deleted:** This indicates that

**Deleted:** While the drivers of ocean acidification trends are identified and quantified above,
**Deleted:** the
**Deleted:** increase in

Likewise, anaerobic remineralization produces alkalinity (Cai et al., 2011). In the sediment of the Bay of Villefranche, sulfate reduction coupled with precipitation of sulfide minerals is the dominant anoxic mineralization pathway (Gaillard et al., 1989). An increase in these processes would explain the observed increase in $A_T$ and $C_T$, but as trends were slower at 50 m compared to 1 m, this would suggest the dominance of a process taking place in surface waters.

In the upper water column at Point B, changes in biological processes are unlikely to explain the observed trends in $A_T$ and $C_T$. For example, the concentration of chlorophyll-a, a proxy of primary production, has decreased since 1995, nutrients increased, and phytoplankton blooms have shifted towards earlier dates in the year (Irisson et al., 2012). While a decrease in net primary production could drive $C_T$ trends, the observed increase in $NO_3^-$ and $PO_4^{3-}$ would cause a small decrease in $A_T$ (Wolf-Gladrow et al., 2007). Stimulated community respiration could result from warming waters but enhanced remineralization would cause a decrease in $A_T$ (Wolf-Gladrow et al., 2007).

The lack of salinity change at the surface excludes additional processes as drivers of $A_T$ and $C_T$ increase at Point B. For example, increased summertime evaporation (concentration effect) and reduced freshwater input (decreased dilution effect) would both be expected to cause an increase in salinity, which was not observed. Increased input of Eastern Mediterranean Sea waters could increase $A_T$, but this is unlikely as this water mass flows much deeper than Point B (Millot and Taupier-Letage, 2005).

Instead, the observed changes in $A_T$ and $C_T$ could be due to increased limestone weathering which would increase the input of $A_T$ from land to the sea via rivers and groundwater. Rivers contribute both $A_T$ and $C_T$ to the Mediterranean Sea (Copin-Montégut, 1993; Tamše et al., 2015). River $A_T$ originates from erosion and is correlated with bedrock composition (e.g., McGrath et al., 2016). Positive trends in river $A_T$ have been documented in

North America and occur via a number of processes including: (1) the interplay of rainfall and land-use (Raymond and Cole, 2003), (2) anthropogenic limestone addition used to enhance agriculture soil pH (Oh and Raymond, 2006; Stets et al., 2014) and freshwater pH (Clair and Hindar, 2005), and (3) potentially indirect effects of anthropogenic $CO_2$ on groundwater $CO_2$-acidification and weathering (Macpherson et al., 2008). Such, and other, processes were hypothesized to have driven $A_T$ changes in the Baltic Sea (Müller et al., 2016). There, an increase in $A_T$ of 3.4 µmol $kg^{-1}$ $yr^{-1}$ was observed from 1995 to 2014 (mean salinity = 7). In contrast to Point B, the increase in Baltic Sea $A_T$ was not noticeable at salinity > 30 (Müller et al., 2016).

Deleted: (a.k.a., liming)

Given the above speculations, the simplest plausible mechanisms causing the unexpected $A_T$ and $C_T$ trends would be through increasing $A_T$ of the freshwater end-member of Point B. Local precipitation, however, did not have an influential effect and was not correlated with salinity or $A_T$ (Fig. S1). While submarine groundwater springs can be a significant source of nutrients, $A_T$, and $C_T$ to the ocean (Cai et al., 2003; Slomp and Van Cappellen, 2004), carbonate chemistry contributions of local submarine springs are currently unknown (Gilli, 1995). Signatures of limestone erosion can be observed in $A_T$ of nearby rivers (Var, Paillon, and Roya) but detailed time-series are not available. Likewise, riverine influence at Point B has not been quantified. If river runoff exerts a dominant control on Point B carbonate chemistry, there is a lag effect, as freshwater influence peaked in May but $A_T$ and $C_T$ increased fastest from May through July. Consequently, this hypothesis needs further investigation. Until the source of $A_T$ increase is properly identified, use of this observation in modeling should be implemented with caution.

## 5. Conclusion

Predictions of coastal ocean acidification remain challenging due the complexity of biogeochemical processes occurring at the ocean-land boundary. At the Point B coastal oceanographic station in the NW Mediterranean Sea, surface ocean acidification was due to atmospheric $CO_2$ forcing and rapid warming over the observation period 2007-2015. However, additional trends in $A_T$ and $C_T$ were observed and remain unexplained, but these trends could relate to riverine and groundwater input. The influence of coastal boundary processes influencing seawater $A_T$ and $C_T$ presents a potentially major difference between coastal and offshore changes in ocean chemistry. This study highlights the importance of considering other anthropogenic influences in the greater land-sea region that may contribute to coastal biogeochemical cycles (*sensu* Duarte et al. 2013) and alter projections of anthropogenic change in near-shore waters.

**Deleted:** monitoring

**Comment [LK19]:** #17

**Deleted:** a

**Data availability –** Time-series data from Point B are available at Pangaea® (doi: 10.1594/PANGAEA.727120)

**Author contribution** – JPG initiated the study, LM supervised data collection, SA performed SeaFET deployments and calibration, JPG and LK designed and JPG conducted statistical analyses, and LK prepared the manuscript with contributions from all authors.

**Competing interests** - The authors declare that they have no conflict of interest.

**Acknowledgements –** Thanks are due to the Service d'Observation Rade de Villefranche (SO-Rade) of the Observatoire Océanologique and the Service d'Observation en Milieu Littoral (SOMLIT/CNRS-INSU) for their kind permission to use the Point B data. Discrete samples were analyzed for $C_T$ and $A_T$ by the *Service National d'Analyse des Paramètres*

*Océaniques du CO2*. The authors thank Jean-Yves Carval, Anne-Marie Corre, Maïa Durozier, Ornella Passafiume and Frank Petit for sampling assistance, to Steeve Comeau and Alice Webb for help with data analysis, and to Bernard Gentili for producing Fig. 1. Atmospheric $CO_2$ data from Plateau Rosa was collected by Ricerca sul Sistema Energetico (RSE S.p.A.); we are grateful for their contribution. We acknowledge L. Coppola for providing DYFAMED data (Coppola et al., 2016) and Météo-France for supplying the meteorological data and the HyMeX database teams (ESPRI/IPSL and SEDOO/Observatoire Midi-Pyrenees) for their help in accessing them. The *Agence de l'Eau Rhône-Méditerranée-Corse* kindly provided data on the chemistry of local rivers. Alexandre Dano, Gilles Dandec and Dominique Chassagne provided the high-resolution bathymetric data for the volume estimate of the Bay. We are grateful for helpful comments from Nicolas Metzl on the manuscript and those from two anonymous reviewers. This work is a contribution to the European Project on Ocean Acidification (EPOCA; contract # 211384) and the MedSeA project (contract # 265103), which received funding from the European Community's Seventh Framework Programme, and to the United States National Science Foundation Ocean Sciences Postdoctoral Research Fellowship (OCE-1521597) awarded to LK.

**References**

Álvarez, M., Sanleón-Bartolomé, H., Tanhua, T., Mintrop, L., Luchetta, A., Cantoni, C., Schroeder, K., and Civitarese, G.: The $CO_2$ system in the Mediterranean Sea: a basin wide perspective, Ocean Sci., 10, 69-92, 10.5194/os-10-69-2014, 2014.

Aminot, A., and Kérouel, R.: Dosage automatique des nutriments dans les eaux marines: méthodes d'analyse en milieu marin, edited by: Ifremer, 188 pp., 2007.

602 Barbier, E. B., Hacker, S. D., Kennedy, C., Koch, E. W., Stier, A. C., and Silliman, B. R.:
603 The value of estuarine and coastal ecosystem services, Ecol. Monogr., 81, 169-193,
604 10.1890/10-1510.1, 2011.
605 Bates, N. R., Astor, Y. M., Church, M. J., Currie, K., Dore, J. E., González-Dávila, M.,
606 Lorenzoni, L., Muller-Karger, F., Olafsson, J., and Santana-Casiano, J. M.: A time-series
607 view of changing ocean chemistry due to ocean uptake of anthropogenic $CO_2$ and ocean
608 acidification, Oceanography, 27, 126-141, 2014.
609 Borges, A. V., and Gypens, N.: Carbonate chemistry in the coastal zone responds more
610 strongly to eutrophication than ocean acidification, Limnol. Oceanogr., 55, 346-353,
611 10.4319/lo.2010.55.1.0346, 2010.
612 Bresnahan, P. J., Martz, T. R., Takeshita, Y., Johnson, K. S., and LaShomb, M.: Best
613 practices for autonomous measurement of seawater pH with the Honeywell Durafet,
614 Methods Oceangr., 9, 44-60, 2014.
615 Cai, W.-J., Wang, Y., Krest, J., and Moore, W. S.: The geochemistry of dissolved inorganic
616 carbon in a surficial groundwater aquifer in North Inlet, South Carolina, and the carbon
617 fluxes to the coastal ocean, Geochim. Cosmochim. Acta, 67, 631-639, 10.1016/S0016-
618 7037(02)01167-5, 2003.
619 Cai, W.-J., Hu, X., Huang, W.-J., Murrell, M. C., Lehrter, J. C., Lohrenz, S. E., Chou, W.-C.,
620 Zhai, W., Hollibaugh, J. T., Wang, Y., Zhao, P., Guo, X., Gundersen, K., Dai, M., and
621 Gong, G.-C.: Acidification of subsurface coastal waters enhanced by eutrophication, Nat.
622 Geosci., 4, 766-770, 10.1038/ngeo1297, 2011.
623 Clair, T. A., and Hindar, A.: Liming for the mitigation of acid rain effects in freshwaters: a
624 review of recent results, Environ. Rev., 13, 91-128, 10.1139/a05-009, 2005.
625 Copin-Montégut, C.: Alkalinity and carbon budgets in the Mediterranean Sea, Global
626 Biogeochem. Cycles, 7, 915-925, 10.1029/93GB01826, 1993.

627 Copin-Montégut, C., and Bégovic, M.: Distributions of carbonate properties and oxygen
628 along the water column (0–2000 m) in the central part of the NW Mediterranean Sea
629 (Dyfamed site): influence of winter vertical mixing on air–sea $CO_2$ and $O_2$ exchanges,
630 Deep-Sea Res. II, 49, 2049-2066, 10.1016/S0967-0645(02)00027-9, 2002.
631 Coppola, L., Diamond Riquier, E., and Carval, T.: Dyfamed observatory data, SEANOE,
632 10.17882/43749, 2016.
633 Cossarini, G., Lazzari, P., and Solidoro, C.: Spatiotemporal variability of alkalinity in the
634 Mediterranean Sea, Biogeosciences, 12, 1647-1658, 10.5194/bg-12-1647-2015, 2015.
635 Costanza, R., d'Arge, R., de Groot, R., Farber, S., Grasso, M., Hannon, B., Limburg, K.,
636 Naeem, S., O'Neill, R. V., Paruelo, J., Raskin, R. G., Sutton, P., and van den Belt, M.:
637 The value of the world's ecosystem services and natural capital, Nature, 387, 253-260,
638 1997.
639 De Carlo, E. H., Mousseau, L., Passafiume, O., Drupp, P. S., and Gattuso, J.-P.: Carbonate
640 chemistry and air–sea $CO_2$ flux in a NW Mediterranean bay over a four-year period:
641 2007–2011, Aquatic Geochemistry, 19, 399-442, 10.1007/s10498-013-9217-4, 2013.
642 Dickson, A.: The carbon dioxide system in seawater: equilibrium chemistry and
643 measurements, in: Guide to best practices for ocean acidification research and data
644 reporting, edited by: Fabry, V. J., Hansson, L., and Gattuso, J.-P., Luxembourg:
645 Publications Office of the European Union, 17-40, 2010.
646 Dickson, A. G., and Riley, J. P.: The effect of analytical error on the evaluation of the
647 components of the aquatic carbon-dioxide system, Mar. Chem., 6, 77-85, 10.1016/0304-
648 4203(78)90008-7, 1978.
649 Dickson, A. G.: Standard potential of the reaction: $AgCl(s) + 1/2\ H_2(g) = Ag(s) + HCl(aq)$,
650 and and the standard acidity constant of the ion $HSO_4^-$ in synthetic sea water from 273.15

651 to 318.15 K, The Journal of Chemical Thermodynamics, 22, 113-127, 10.1016/0021-
652 9614(90)90074-Z, 1990.
653 Dickson, A. G., Sabine, C. L., and Christian, J. R.: Guide to best practices for ocean $CO_2$
654 measurements, PICES Special Publication, 3, 191 pp., 2007.
655 DOE: Handbook of methods for the analysis of the various parameters of the carbon dioxide
656 system in sea water, Carbon Dioxide Information Analysis Center, Oak Ridge National
657 Laboratory, 1994.
658 Doney, S. C., Fabry, V. J., Feely, R. A., and Kleypas, J. A.: Ocean acidification: the other
659 $CO_2$ problem, Ann. Rev. Mar. Sci., 1, 169-192, 10.1146/annurev.marine.010908.163834,
660 2009.
661 Duarte, C. M., Hendriks, I. E., Moore, T. S., Olsen, Y. S., Steckbauer, A., Ramajo, L.,
662 Carstensen, J., Trotter, J. A., and McCulloch, M.: Is ocean acidification an open-ocean
663 syndrome? Understanding anthropogenic impacts on seawater pH, Estuaries and Coasts,
664 36, 221-236, 10.1007/s12237-013-9594-3, 2013.
665 Edmond, J. M.: High precision determination of titration alkalinity and total carbon dioxide
666 content of sea water by potentiometric titration, Deep-Sea Research, 17, 737-750,
667 10.1016/0011-7471(70)90038-0, 1970.
668 Feely, R. A., Sabine, C. L., Hernandez-Ayon, J. M., Ianson, D., and Hales, B.: Evidence for
669 upwelling of corrosive "acidified" water onto the continental shelf, Science, 320, 1490-
670 1492, 10.1126/science.1155676, 2008.
671 Feely, R. A., Alin, S. R., Newton, J., Sabine, C. L., Warner, M., Devol, A., Krembs, C., and
672 Maloy, C.: The combined effects of ocean acidification, mixing, and respiration on pH
673 and carbonate saturation in an urbanized estuary, Estuar. Coast. Shelf Sci., 88,
674 10.1016/j.ecss.2010.05.004, 2010.

675 Flecha, S., Pérez, F. F., García-Lafuente, J., Sammartino, S., Ríos, A. F., and Huertas, I. E.:
676 Trends of pH decrease in the Mediterranean Sea through high frequency observational
677 data: indication of ocean acidification in the basin, Sci. Rep., 5, 16770,
678 10.1038/srep16770, 2015.
679 Gaillard, J.-F., Pauwels, H., and Michard, G.: Chemical diagenesis in coastal marine
680 sediments, Oceanol. Acta, 12, 175-187, 1989.
681 García-Ibáñez, M. I., Zunino, P., Fröb, F., Carracedo, L. I., Ríos, A. F., Mercier, H., Olsen,
682 A., and Pérez, F. F.: Ocean acidification in the subpolar North Atlantic: rates and
683 mechanisms controlling pH changes, Biogeosciences, 13, 3701-3715, 10.5194/bg-13-
684 3701-2016, 2016.
685 Gattuso, J.-P., Epitalon, J.-M., and Lavigne, H.: seacarb: Seawater Carbonate Chemistry. R
686 package version 3.1.1 https://cran.r-project.org/package=seacarb, 2016.
687 Gattuso, J. P., and Hansson, L.: Ocean acidification, Oxford University Press, Oxford, 2011.
688 Gilli, E.: Etude des sources karstiques sous-marines et littorales des Alpes Maritimes entre
689 Menton et Nice, 41, 1995.
690 Halpern, B. S., Walbridge, S., Selkoe, K. A., Kappel, C. V., Micheli, F., D'Agrosa, C., Bruno,
691 J. F., Casey, K. S., Ebert, C., and Fox, H. E.: A global map of human impact on marine
692 ecosystems, Science, 319, 948-952, 2008.
693 Hofmann, G. E., Smith, J. E., Johnson, K. S., Send, U., Levin, L. A., Micheli, F., Paytan, A.,
694 Price, N. N., Peterson, B., Takeshita, Y., Matson, P. G., Crook, E. D., Kroeker, K. J.,
695 Gambi, M. C., Rivest, E. B., Frieder, C. A., Yu, P. C., and Martz, T. R.: High-frequency
696 dynamics of ocean pH: a multi-ecosystem comparison, PLoS One, 6, e28983,
697 10.1371/journal.pone.0028983, 2011.

698 Howes, E. L., Stemmann, L., Assailly, C., Irisson, J. O., Dima, M., Bijma, J., and Gattuso, J.
699 P.: Pteropod time series from the North Western Mediterranean (1967-2003): impacts of
700 pH and climate variability, Mar. Ecol. Prog. Ser., 531, 193-206, 2015.
701 Ingrosso, G., Giani, M., Comici, C., Kralj, M., Piacentino, S., De Vittor, C., and Del Negro,
702 P.: Drivers of the carbonate system seasonal variations in a Mediterranean gulf, Estuar.
703 Coast. Shelf Sci., 168, 58-70, 10.1016/j.ecss.2015.11.001, 2016.
704 Irisson, J.-O., Webb, A., Passafiume, O., and Mousseau, L.: Detecting hydrologic variations
705 in a long term monitoring time series, Europole Mer Gordon-like conference "Time-series
706 analysis in marine science and application for industry", Brest, France, 17-21 Sept 2012,
707 2012.
708 Jiang, Z.-P., Tyrrell, T., Hydes, D. J., Dai, M., and Hartman, S. E.: Variability of alkalinity
709 and the alkalinity-salinity relationship in the tropical and subtropical surface ocean,
710 Global Biogeochem. Cycles, 28, 729-742, 10.1002/2013GB004678, 2014.
711 Kapsenberg, L., Kelley, A. L., Shaw, E. C., Martz, T. R., and Hofmann, G. E.: Near-shore
712 Antarctic pH variability has implications for biological adaptation to ocean acidification,
713 Sci. Rep., 5, 9638, 10.1038/srep09638, 2015.
714 Kapsenberg, L., and Hofmann, G. E.: Ocean pH time-series and drivers of variability along
715 the northern Channel Islands, California, USA, Limnol. Oceanogr., 61, 953-968,
716 10.1002/lno.10264, 2016.
717 Krasakopoulou, E., Souvermezoglou, E., and Goyet, C.: Anthropogenic $CO_2$ fluxes in the
718 Otranto Strait (E. Mediterranean) in February 1995, Deep-Sea Res. I, 58, 1103-1114,
719 10.1016/j.dsr.2011.08.008, 2011.
720 Lacoue-Labarthe, T., Nunes, P. A. L. D., Ziveri, P., Cinar, M., Gazeau, F., Hall-Spencer, J.
721 M., Hilmi, N., Moschella, P., Safa, A., Sauzade, D., and Turley, C.: Impacts of ocean

722 acidification in a warming Mediterranean Sea: An overview, Regional Studies in Marine
723 Science, 5, 1-11, 10.1016/j.rsma.2015.12.005, 2016.
724 Le Quéré, C., Andrew, R. M., Canadell, J. G., Sitch, S., Korsbakken, J. I., Peters, G. P.,
725 Manning, A. C., Boden, T. A., Tans, P. P., Houghton, R. A., Keeling, R. F., Alin, S.,
726 Andrews, O. D., Anthoni, P., Barbero, L., Bopp, L., Chevallier, F., Chini, L. P., Ciais, P.,
727 Currie, K., Delire, C., Doney, S. C., Friedlingstein, P., Gkritzalis, T., Harris, I., Hauck, J.,
728 Haverd, V., Hoppema, M., Klein Goldewijk, K., Jain, A. K., Kato, E., Körtzinger, A.,
729 Landschützer, P., Lefèvre, N., Lenton, A., Lienert, S., Lombardozzi, D., Melton, J. R.,
730 Metzl, N., Millero, F., Monteiro, P. M. S., Munro, D. R., Nabel, J. E. M. S., Nakaoka, S.
731 I., O'Brien, K., Olsen, A., Omar, A. M., Ono, T., Pierrot, D., Poulter, B., Rödenbeck, C.,
732 Salisbury, J., Schuster, U., Schwinger, J., Séférian, R., Skjelvan, I., Stocker, B. D.,
733 Sutton, A. J., Takahashi, T., Tian, H., Tilbrook, B., van der Laan-Luijkx, I. T., van der
734 Werf, G. R., Viovy, N., Walker, A. P., Wiltshire, A. J., and Zaehle, S.: Global Carbon
735 Budget 2016, Earth Syst. Sci. Data, 8, 605-649, 10.5194/essd-8-605-2016, 2016.
736 Lee, K., Kim, T.-W., Byrne, R. H., Millero, F. J., Feely, R. A., and Liu, Y.-M.: The universal
737 ratio of boron to chlorinity for the North Pacific and North Atlantic oceans, Geochim.
738 Cosmochim. Acta, 74, 1801-1811, 10.1016/j.gca.2009.12.027, 2010.
739 Lee, K., Sabine, C. L., Tanhua, T., Kim, T.-W., Feely, R. A., and Kim, H.-C.: Roles of
740 marginal seas in absorbing and storing fossil fuel $CO_2$, Energy & Environmental Science,
741 4, 1133-1146, 10.1039/C0EE00663G, 2011.
742 Lejeusne, C., Chevaldonné, P., Pergent-Martini, C., Boudouresque, C. F., and Pérez, T.:
743 Climate change effects on a miniature ocean: the highly diverse, highly impacted
744 Mediterranean Sea, Trends Ecol. Evol., 25, 250-260,
745 http://dx.doi.org/10.1016/j.tree.2009.10.009, 2010.

746 Luchetta, A., Cantoni, C., and Catalano, G.: New observations of $CO_2$-induced acidification
747 in the northern Adriatic Sea over the last quarter century, Chem. Ecol., 26, 1-17,
748 10.1080/02757541003627688, 2010.
749 Lueker, T. J., Dickson, A. G., and Keeling, C. D.: Ocean $pCO_2$ calculated from dissolved
750 inorganic carbon, alkalinity, and equations for $K_1$ and $K_2$: validation based on laboratory
751 measurements of $CO_2$ in gas and seawater at equilibrium, Mar. Chem., 70, 105-119,
752 10.1016/S0304-4203(00)00022-0, 2000.
753 Macpherson, G. L., Roberts, J. A., Blair, J. M., Townsend, M. A., Fowle, D. A., and Beisner,
754 K. R.: Increasing shallow groundwater $CO_2$ and limestone weathering, Konza Prairie,
755 USA, Geochim. Cosmochim. Acta, 72, 5581-5599, 10.1016/j.gca.2008.09.004, 2008.
756 Marcellin Yao, K., Marcou, O., Goyet, C., Guglielmi, V., Touratier, F., and Savy, J.-P.: Time
757 variability of the north-western Mediterranean Sea pH over 1995–2011, Mar. Environ.
758 Res., 116, 51-60, 10.1016/j.marenvres.2016.02.016, 2016.
759 McGrath, T., McGovern, E., Cave, R. R., and Kivimäe, C.: The inorganic carbon chemistry
760 in coastal and shelf waters around Ireland, Estuaries and Coasts, 39, 27-39,
761 10.1007/s12237-015-9950-6, 2016.
762 Meier, K. J. S., Beaufort, L., Heussner, S., and Ziveri, P.: The role of ocean acidification in
763 *Emiliania huxleyi* coccolith thinning in the Mediterranean Sea, Biogeosciences, 11, 2857-
764 2869, 10.5194/bg-11-2857-2014, 2014.
765 The MerMex Group, Durrieu de Madron, X., Guieu, C., Sempéré, R., Conan, P., Cossa, D.,
766 D'Ortenzio, F., Estournel, C., Gazeau, F., Rabouille, C., Stemmann, L., Bonnet, S., Diaz,
767 F., Koubbi, P., Radakovitch, O., Babin, M., Baklouti, M., Bancon-Montigny, C., Belviso,
768 S., Bensoussan, N., Bonsang, B., Bouloubassi, I., Brunet, C., Cadiou, J. F., Carlotti, F.,
769 Chami, M., Charmasson, S., Charrière, B., Dachs, J., Doxaran, D., Dutay, J. C., Elbaz-
770 Poulichet, F., Eléaume, M., Eyrolles, F., Fernandez, C., Fowler, S., Francour, P.,

Gaertner, J. C., Galzin, R., Gasparini, S., Ghiglione, J. F., Gonzalez, J. L., Goyet, C., Guidi, L., Guizien, K., Heimbürger, L. E., Jacquet, S. H. M., Jeffrey, W. H., Joux, F., Le Hir, P., Leblanc, K., Lefèvre, D., Lejeusne, C., Lemé, R., Loÿe-Pilot, M. D., Mallet, M., Méjanelle, L., Mélin, F., Mellon, C., Mérigot, B., Merle, P. L., Migon, C., Miller, W. L., Mortier, L., Mostajir, B., Mousseau, L., Moutin, T., Para, J., Pérez, T., Petrenko, A., Poggiale, J. C., Prieur, L., Pujo-Pay, M., Pulido, V., Raimbault, P., Rees, A. P., Ridame, C., Rontani, J. F., Ruiz Pino, D., Sicre, M. A., Taillandier, V., Tamburini, C., Tanaka, T., Taupier-Letage, I., Tedetti, M., Testor, P., Thébault, H., Thouvenin, B., Touratier, F., Tronczynski, J., Ulses, C., Van Wambeke, F., Vantrepotte, V., Vaz, S., and Verney, R.: Marine ecosystems' responses to climatic and anthropogenic forcings in the Mediterranean, Prog. Oceanogr., 91, 97-166, 10.1016/j.pocean.2011.02.003, 2011.

Millot, C., and Taupier-Letage, I.: Circulation in the Mediterranean Sea, in: The Mediterranean Sea, edited by: Saliot, A., Springer Berlin Heidelberg, Berlin, Heidelberg, 29-66, 2005.

Moulin, E., Jordens, A., and Wollast, R.: Influence of the aerobic bacterial respiration on the early dissolution of carbonates in coastal sediments, in: Progress in Belgian Oceanographic Research: Proceedings of a Symposium Held at the Palace of Academies Brussels, edited by: Van Grieken, R., and Wollast, R., Brussels, 196-208, 1985.

Müller, J. D., Schneider, B., and Rehder, G.: Long-term alkalinity trends in the Baltic Sea and their implications for $CO_2$-induced acidification, Limnol. Oceanogr., 10.1002/lno.10349, 2016.

Oh, N.-H., and Raymond, P. A.: Contribution of agricultural liming to riverine bicarbonate export and $CO_2$ sequestration in the Ohio River basin, Global Biogeochem. Cycles, 20, GB3012, 10.1029/2005GB002565, 2006.

795 Omstedt, A., Edman, M., Claremar, B., and Rutgersson, A.: Modelling the contributions to
796 marine acidification from deposited $SO_x$, $NO_x$, and $NH_x$ in the Baltic Sea: Past and
797 present situations, Cont. Shelf Res., 111, Part B, 234-249, 10.1016/j.csr.2015.08.024,
798 2015.
799 Palmiéri, J., Orr, J., Dutay, J., Béranger, K., Schneider, A., Beuvier, J., and Somot, S.:
800 Simulated anthropogenic $CO_2$ storage and acidification of the Mediterranean Sea,
801 Biogeosciences, 12, 781-802, 2015.
802 Parravicini, V., Mangialajo, L., Mousseau, L., Peirano, A., Morri, C., Montefalcone, M.,
803 Francour, P., Kulbicki, M., and Bianchi, C. N.: Climate change and warm-water species
804 at the north-western boundary of the Mediterranean Sea, Mar. Ecol., 36, 897-909,
805 10.1111/maec.12277, 2015.
806 Perez, F. F., and Fraga, F.: The pH measurements in seawater on the NBS scale, Mar. Chem.,
807 21, 315-327, 10.1016/0304-4203(87)90054-5, 1987.
808 Pörtner, H.-O., Karl, D., Boyd, P. W., Cheung, W., Lluch-Cota, S. E., Nojiri, Y., Schmidt, D.
809 N., and Zavialov, P.: Ocean systems, in: Climate Change 2014: Impacts, Adaptation, and
810 Vulnerability. Part A: Global and Sectoral Aspects. Contribution of Working Group II to
811 the Fifth Assessment Report of the Intergovernmental Panel on Climate Change, edited
812 by: Field, C. B., Barros, V. R., Dokken, D. J., Mach, K. J., Mastrandrea, M. D., Bilir, T.
813 E., Chatterjee, M., Ebi, K. L., Estrada, Y. O., Genova, R. C., Girma, B., Kissel, E. S.,
814 Levy, A. N., MacCracken, S., Mastrandrea, P. R., and L.L.White, Cambridge University
815 Press, Cambridge, United Kingdom and New York, NY, USA, 411-484, 2014.
816 Provoost, P., van Heuven, S., Soetaert, K., Laane, R. W. P. M., and Middelburg, J. J.:
817 Seasonal and long-term changes in pH in the Dutch coastal zone, Biogeosciences, 7,
818 3869-3878, 10.5194/bg-7-3869-2010, 2010.

819 Raymond, P. A., and Cole, J. J.: Increase in the export of alkalinity from North America's
820 largest river, Science, 301, 88-91, 2003.
821 Rhein, M., Rintoul, S. R., Aoki, S., Campos, E., Chambers, D., Feely, R. A., Gulev, S.,
822 Johnson, G. C., Josey, S. A., A. Kostianoy, Mauritzen, C., Roemmich, D., Talley, L. D.,
823 and Wang, F.: Observations: Ocean, in: Climate Change 2013: The Physical Science
824 Basis. Contribution of Working Group I to the Fifth Assessment Report of the
825 Intergovernmental Panel on Climate Change, edited by: Stocker, T. F., Qin, D., Plattner,
826 G.-K., Tignor, M., Allen, S. K., Boschung, J., Nauels, A., Xia, Y., Bex, V., and Midgley,
827 P. M., Cambridge University Press, Cambridge, United Kingdom and New York, NY,
828 USA., 2013.
829 Schneider, A., Wallace, D. W. R., and Körtzinger, A.: Alkalinity of the Mediterranean Sea,
830 Geophys. Res. Lett., 34, L15608, 10.1029/2006GL028842, 2007.
831 Schneider, A., Tanhua, T., Körtzinger, A., and Wallace, D. W. R.: High anthropogenic
832 carbon content in the eastern Mediterranean, J. Geophys. Res., 115, C12050,
833 10.1029/2010JC006171, 2010.
834 Slomp, C. P., and Van Cappellen, P.: Nutrient inputs to the coastal ocean through submarine
835 groundwater discharge: controls and potential impact, Journal of Hydrology, 295, 64-86,
836 10.1016/j.jhydrol.2004.02.018, 2004.
837 Stets, E. G., Kelly, V. J., and Crawford, C. G.: Long-term trends in alkalinity in large rivers
838 of the conterminous US in relation to acidification, agriculture, and hydrologic
839 modification, Sci. Total Environ., 488–489, 280-289, 10.1016/j.scitotenv.2014.04.054,
840 2014.
841 Tamše, S., Ogrinc, N., Walter, L. M., Turk, D., and Faganeli, J.: River sources of dissolved
842 inorganic carbon in the Gulf of Trieste (N Adriatic): stable carbon isotope evidence,
843 Estuaries and Coasts, 38, 151-164, 10.1007/s12237-014-9812-7, 2015.

844 Tanhua, T., Bates, N. R., and Körtzinger, A.: The marine carbon cycle and ocean
845 anthropogenic $CO_2$ inventories, in: Ocean Circulation and Climate: A 21st Century
846 Perspective. 2nd Ed, edited by: Siedler, G., Griffies, S., Gould, J., and Church, J., 103,
847 Academic Press, 787-816, 2013.
848 Team, R. C.: R: A language and environment for statistical computing. R Foundation for
849 Statistical Computing, Vienna, Austria. https://www.r-project.org/, 2016.
850 Touratier, F., and Goyet, C.: Impact of the Eastern Mediterranean Transient on the
851 distribution of anthropogenic $CO_2$ and first estimate of acidification for the Mediterranean
852 Sea, Deep-Sea Res. I, 58, 1-15, 10.1016/j.dsr.2010.10.002, 2011.
853 Touratier, F., Goyet, C., Houpert, L., de Madron, X. D., Lefèvre, D., Stabholz, M., and
854 Guglielmi, V.: Role of deep convection on anthropogenic $CO_2$ sequestration in the Gulf
855 of Lions (northwestern Mediterranean Sea), Deep-Sea Res. I, 113, 33-48,
856 10.1016/j.dsr.2016.04.003, 2016.
857 Vargas, C. A., Contreras, P. Y., Pérez, C. A., Sobarzo, M., Saldías, G. S., and Salisbury, J.:
858 Influences of riverine and upwelling waters on the coastal carbonate system off Central
859 Chile and their ocean acidification implications, Journal of Geophysical Research:
860 Biogeosciences, 121, 1468-1483, 10.1002/2015JG003213, 2016.
861 Wolf-Gladrow, D. A., Zeebe, R. E., Klaas, C., Körtzinger, A., and Dickson, A. G.: Total
862 alkalinity: The explicit conservative expression and its application to biogeochemical
863 processes, Mar. Chem., 106, 287-300, 10.1016/j.marchem.2007.01.006, 2007.
864 Wootton, J. T., Pfister, C. A., and Forester, J. D.: Dynamic patterns and ecological impacts of
865 declining ocean pH in a high-resolution multi-year dataset, Proc. Natl. Acad. Sci., 105,
866 18848-18853, 2008.
867 Wootton, J. T., and Pfister, C. A.: Carbon system measurements and potential climatic
868 drivers at a site of rapidly declining ocean pH, PLoS One, 7, e53396, 2012.

869 **Table 1.** Previous estimates or documentation of pH change (ΔpH**)** in the Mediterranean Sea.

870 'Total' indicates estimates made for the whole Mediterranean Sea. TrOCA is the 'Tracer

871 combining Oxygen, inorganic Carbon, and total Alkalinity' method, NR means 'not

872 reported', and PI is 'pre-industrial era'. *indicates studies where the reported pH change was

873 assumed to be at *in situ* temperatures.

| ***Region*** | ***Site*** | ***Method*** | ***Study period*** | ***pH scale*** | ***°C*** | ***ΔpH yr$^{-1}$ ± SE*** | ***Total ΔpH*** | ***Reference*** |
|---|---|---|---|---|---|---|---|---|
| NW | Point B, 1 m | time-series, anomaly | 2007-2015 | total | *in situ* | -0.0028 ± 0.0003 | -0.0252 | This study |
| NW | Point B, 1 m | time-series, anomaly | 2007-2015 | total | 25 | -0.0017 ± 0.0002 | -0.0153 | This study |
| NW | Point B | model | 1967-2003 | total | *in situ* | -0.0014 | -0.05 | Howes et al. (2015) |
| NW | DYFAMED | time-series, observed | 1995-2011 | seawater | *in situ* | -0.003 ± 0.001 | -0.051 | Marcellin Yao et al. (2016) |
| NW | DYFAMED | time-series comparison | 1998-2000, 2003-2005 | seawater | *in situ** | - | -0.02 | Meier et al. (2014) |
| NW | Gulf of Lion | TrOCA | PI-2011 | NR | *in situ** | - | -0.15 to -0.11 | Touratier et al. (2016) |
| East | N Adriatic Sea | cruise comparison | 1983, 2008 | total | 25 | -0.0025 | -0.063 | Luchetta et al. (2010) |
| East | Otranto Strait | TrOCA | PI-1995 | seawater | 25 | - | < -0.1 to -0.05, ± 0.014 | Krasakopoulou et al. (2011) |
| Total | Full profile | TrOCA | PI-2001 | NR | *in situ** | - | -0.14 to -0.05 | Touratier and Goyet (2011) |
| Total | Bottom waters | model | 1800-2001 | total | *in situ** | - | -0.06 to -0.005 | Palmiéri et al. (2015) |
| Total | Surface waters | model | 1800-2001 | total | *in situ** | - | -0.084 ± 0.001 | Palmiéri et al. (2015) |
| Gibraltar Strait | Espartel sill | pH, $pCO_2$ sensors | 2012-2015 | total | 25 | -0.0044 ± 0.00006 | - | Flecha et al. (2015) |

874

875

**Table 2.** Time-series anomaly regression analyses on seawater carbonate chemistry at Point B for salinity (S), temperature (T), dissolved inorganic carbon ($C_T$), total alkalinity ($A_T$), $pH_T$, $pH_T$ normalized to 25 ºC ($pH_{T25}$), $pCO_2$, calcite ($\Omega_c$) and aragonite ($\Omega_a$) saturation state, and salinity-normalized $A_T$ ($nA_T$) and $C_T$ ($nC_T$), at 1 and 50 m. Slopes represent the change in the variable unit per year. $P$ <<0.001 indicates $p$-values far smaller than 0.001.

| *Depth (m)* | *Variable* | *Slope ± SE* | *Intercept ± SE* | *N* | *F* | *df* | *Slope P* | $R^2$ |
|---|---|---|---|---|---|---|---|---|
| 1 | S | -0.0017 ± 0.0044 | 3.38 ± 8.82 | 417 | 0.147 | 1,415 | 0.702 | 0 |
| | T (ºC) | 0.072 ± 0.022 | -145 ± 44 | 413 | 10.999 | 1,411 | 0.001 | 0.026 |
| | $C_T$ (µmol kg$^{-1}$) | 2.97 ± 0.20 | -5965 ± 400 | 416 | 221.87 | 1,414 | <<0.001 | 0.349 |
| | $A_T$ (µmol kg$^{-1}$) | 2.08 ± 0.19 | -4189 ± 379 | 417 | 122.429 | 1,415 | <<0.001 | 0.228 |
| | $pH_T$ | -0.0028 ± 0.0003 | 5.72 ± 0.66 | 412 | 74.205 | 1,410 | <<0.001 | 0.153 |
| | $pH_{T25}$ | -0.0017 ± 0.0002 | 3.46 ± 0.43 | 412 | 64.204 | 1, 410 | <<0.001 | 0.1354 |
| | $pCO_2$ (µatm) | 3.53 ± 0.39 | -7105 ± 776 | 412 | 83.927 | 1,410 | <<0.001 | 0.17 |
| | $\Omega_c$ | -0.0109 ± 0.0022 | 22.0 ± 4.5 | 412 | 24.08 | 1,410 | <<0.001 | 0.055 |
| | $\Omega_a$ | -0.0064 ± 0.0015 | 12.9 ± 3.1 | 412 | 17.33 | 1,410 | <<0.001 | 0.041 |
| | $nA_T$ (µmol kg$^{-1}$) | 2.20 ± 0.28 | -4425 ± 560 | 412 | 62.34 | 1,410 | <<0.001 | 0.132 |
| | $nC_T$ (µmol kg$^{-1}$) | 3.12 ± 0.29 | -6275 ± 579 | 412 | 117.486 | 1,410 | <<0.001 | 0.223 |
| 50 | S | 0.0063 ± 0.0020 | -12.8 ± 4.1 | 412 | 9.858 | 1, 410 | 0.002 | 0.0235 |
| | T (ºC) | 0.088 ± 0.019 | -177 ± 38 | 408 | 21.927 | 1, 406 | <<0.001 | 0.0512 |
| | $C_T$ (µmol kg$^{-1}$) | 2.16 ± 0.21 | -4344 ± 418 | 411 | 108.105 | 1, 409 | <<0.001 | 0.2091 |
| | $A_T$ (µmol kg$^{-1}$) | 1.59 ± 0.15 | -3192 ± 309 | 412 | 106.947 | 1, 410 | <<0.001 | 0.2069 |
| | $pH_T$ | -0.0026 ± 0.0002 | 5.28 ± 0.50 | 407 | 112.111 | 1, 405 | <<0.001 | 0.2168 |
| | $pH_{T25}$ | -0.0013 ± 0.0003 | 2.55 ± 0.54 | 407 | 21.863 | 1, 405 | <<0.001 | 0.0512 |
| | $pCO_2$ (µatm) | 2.79 ± 0.25 | -5603 ± 501 | 407 | 125.1 | 1, 405 | <<0.001 | 0.236 |
| | $\Omega_c$ | -0.0070 ± 0.0027 | 14.0 ± 5.4 | 407 | 6.648 | 1, 405 | 0.01 | 0.0162 |
| | $\Omega_a$ | -0.0038 ± 0.0019 | 7.6 ± 3.7 | 407 | 4.155 | 1, 405 | 0.042 | 0.0102 |
| | $nA_T$ (µmol kg$^{-1}$) | 1.15 ± 0.13 | -2309 ± 254 | 407 | 82.309 | 1, 405 | <<0.001 | 0.1689 |
| | $nC_T$ (µmol kg$^{-1}$) | 1.82 ± 0.19 | -3661 ± 376 | 407 | 94.98 | 1, 405 | <<0.001 | 0.19 |

883 **Table 3.** Deconvolution of $pH_T$ anomalies ($\frac{dpH_T}{dt}$, units $pH_T$ $yr^{-1}$) at 1 and 50 m.

884 Sensitivity of $pH_T$ with respect to variables ($\frac{\partial pH_T}{\partial var}$), where the variable *var* is either

885 temperature (T), salinity (S), total alkalinity ($A_T$), or dissolved inorganic carbon ($C_T$), was

886 multiplied by the anomaly of *var* ($\frac{dvar}{dt}$, Table 2). SE is standard error and RMSE is root-

887 mean-squared error. Rounding was performed at the end of the calculations, prior to

888 estimating percent contributions.

| ***Depth (m)*** | ***var*** | $\frac{\partial pH_T}{\partial var} \pm SE$ | $\frac{\partial pH_T}{\partial var}\frac{dvar}{dt} \pm RMSE$ | ***Contribution (%)*** | $\frac{dpH_T}{dt} \pm RMSE$ |
|---|---|---|---|---|---|
| 1 | T (ºC) | -0.0153 ± <0.0001 | -0.0011 ± 0.0003 | 41 | -0.0027 ± 0.0005 |
| | S | -0.0117 ± <0.0001 | <0.0001 ± 0.0001 | 0 | |
| | $A_T$ (µmol $kg^{-1}$) | 0.0015 ± <0.0001 | 0.0031 ± 0.0003 | -115 | |
| | $C_T$ (µmol $kg^{-1}$) | -0.0016 ± <0.0001 | -0.0047 ± 0.0003 | 174 | |
| 50 | T (ºC) | -0.0154 ± <0.0001 | -0.0014 ± 0.0003 | 54 | -0.0026 ± 0.0005 |
| | S | -0.0116 ± <0.0001 | -0.0001 ± <0.0001 | 4 | |
| | $A_T$ (µmol $kg^{-1}$) | 0.0015 ± <0.0001 | 0.0024 ± 0.0002 | -92 | |
| | $C_T$ (µmol $kg^{-1}$) | -0.0016 ± <0.0001 | -0.0035 ± 0.0003 | 135 | |

889

**Table 4.** Deconvolution of $pCO_2$ anomalies ($\frac{dpCO_2}{dt}$, µatm $yr^{-1}$) at 1 and 50 m. Details are the same as in Table 3.

| *Depth (m)* | *var* | $\frac{\partial pCO_2}{\partial var} \pm SE$ | $\frac{\partial pCO_2}{\partial var}\frac{dvar}{dt} \pm RMSE$ | *Contribution (%)* | $\frac{dpCO_2}{dt} \pm RMSE$ |
|---|---|---|---|---|---|
| 1 | T (ºC) | 16.49 ± 0.05 | 1.19 ± 0.36 | 37 | 3.23 ± 0.57 |
| | S | 10.14 ± <0.01 | -0.02 ± 0.05 | -1 | |
| | $A_T$ (µmol $kg^{-1}$) | -1.478 ± 0.005 | -3.08 ± 0.28 | -95 | |
| | $C_T$ (µmol $kg^{-1}$) | 1.735 ± 0.006 | 5.14 ± 0.35 | 159 | |
| 50 | T (ºC) | 15.55 ± 0.03 | 1.37 ± 0.29 | 48 | 2.84 ± 0.49 |
| | S | 9.355 ± <0.001 | 0.06 ± 0.02 | 2 | |
| | $A_T$ (µmol $kg^{-1}$) | -1.327 ± 0.002 | -2.11 ± 0.20 | -74 | |
| | $C_T$ (µmol $kg^{-1}$) | 1.629 ± 0.005 | 3.52 ± 0.34 | 124 | |

**Figure 1.** Map of study region in the NW Mediterranean Sea (a), along the North current (b) in the Bay of Villefranche-sur-Mer, France (c). Point B, EOL buoy, and the offshore time-series station DYFAMED are marked. Bathymetric line units are m (c).

Deleted: station

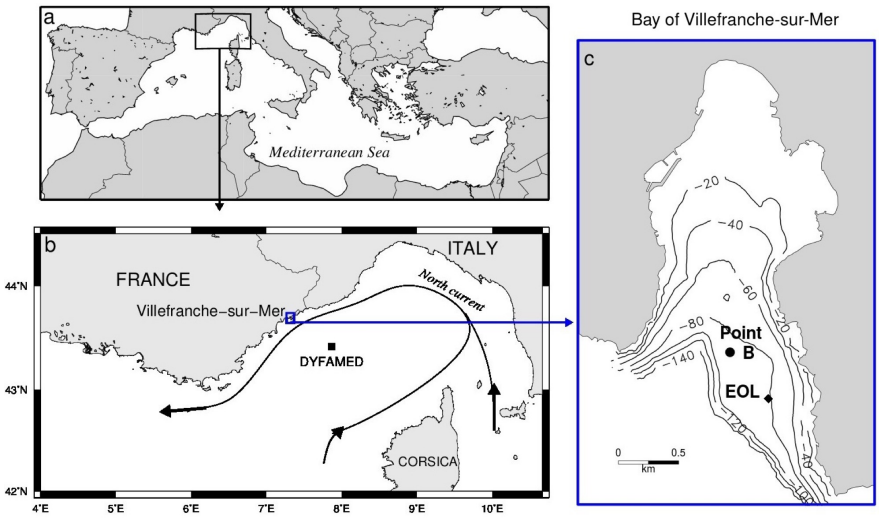

**Figure 2.** Time-series observations (a-g) and anomaly trends (h-n) for temperature, salinity, and seawater carbonate chemistry at Point B, 1 m. Regression slopes are drawn ± SE (in grey) and noted with a star for significance at $\alpha = 0.05$. Variable abbrevations are the same as in Table 2.

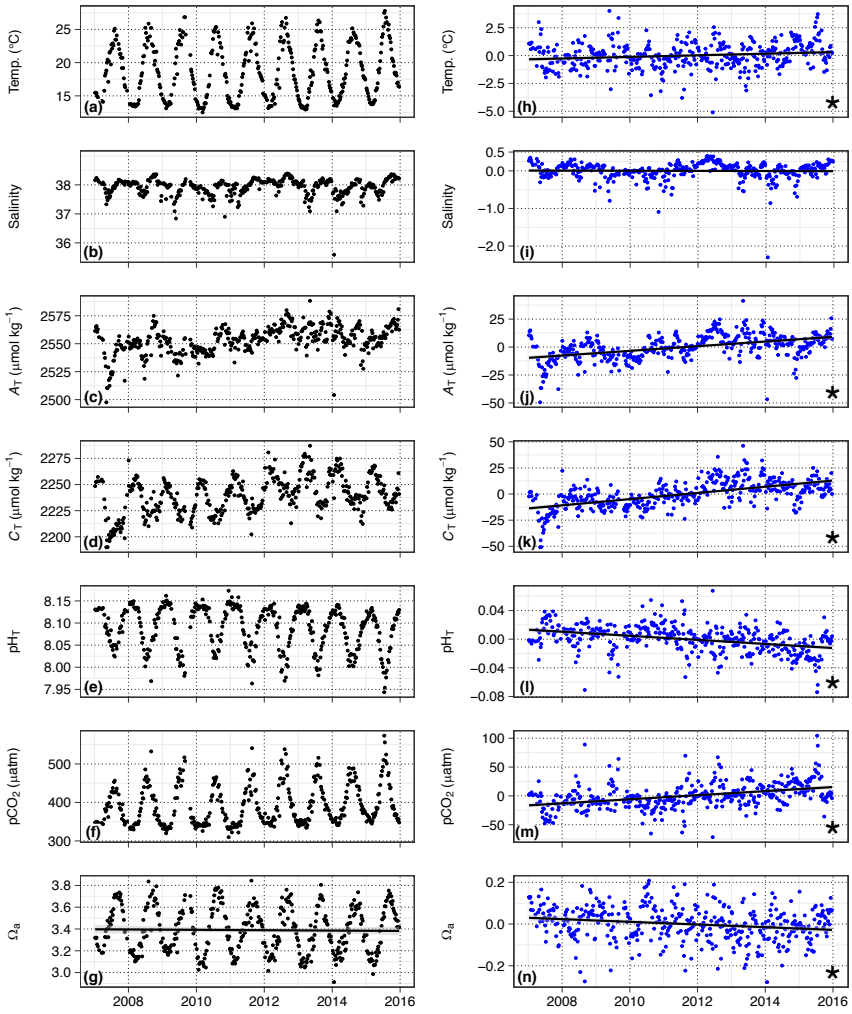

**Figure 3.** Time-series observations (a-g) and anomaly trends (h-n) for temperature, salinity, and seawater carbonate chemistry at Point B, 50 m. Regression slopes are drawn ± SE (in grey) and noted with a star for significance at $\alpha = 0.05$. Variable abbrevations are the same as in Table 2.

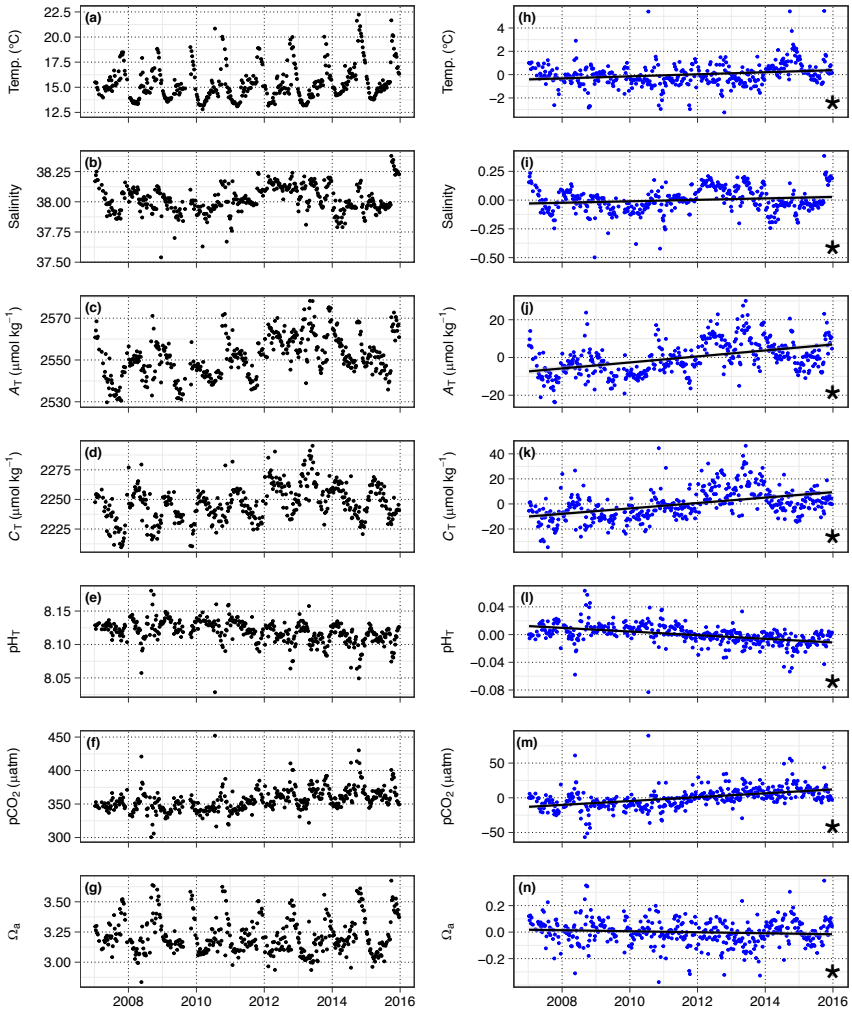


Deleted:

**Figure 4.** Monthly distribution of seawater carbonate chemistry at Point B, 1 m, using a combination of a violin plot showing the relative frequency of the observations (shaded blue area) and a boxplot showing the median, first and third quartiles, as well as outliers (blue).

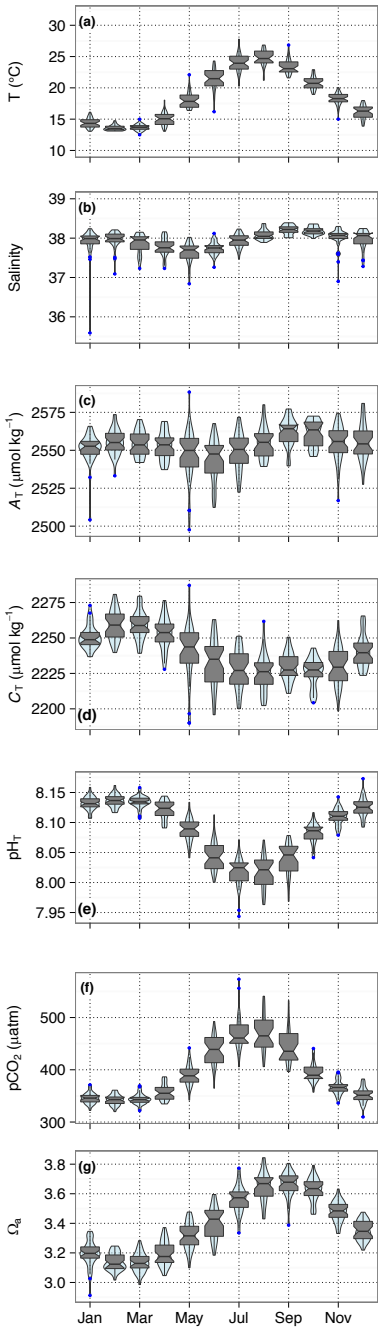

916 **Figure 5.** Monthly trends of total alkalinity ($A_T$, blue) and dissolved inorganic carbon ($C_T$,
917 green) for the period 2007-2015. Errors bars are ± SE of the slope estimate and significance
918 is noted (*) at $\alpha = 0.05$.

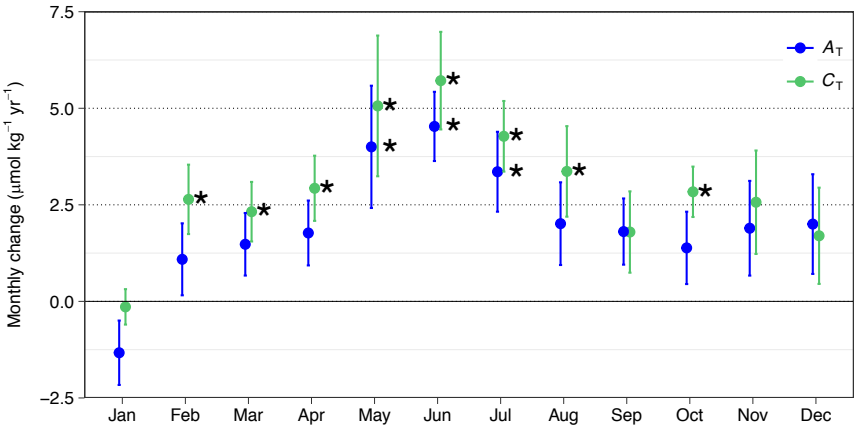


919

**Figure 6.** Salinity and total alkalinity ($A_T$) relationships at Point B for the period 2007-2015, by year, at 1 m. Data points are colored for month.

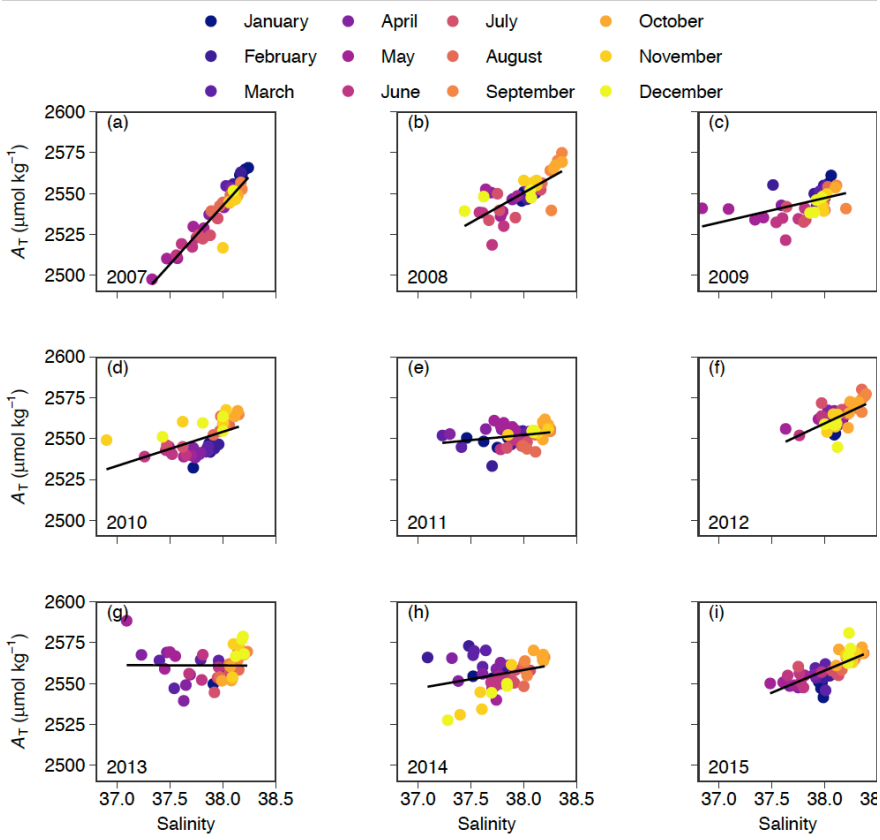

**Figure 7.** Time-series $pH_T$ (a) and temperature (b) from SeaFET pH sensor deployments at EOL, 2 m. Discrete calibration samples are noted in green, and grey vertical lines bracket deployment periods (a). Calibration sample offsets from processed pH time-series are shown in panel (c). Violin and boxplots (see Fig. 4) show diel pH range by month (d), and an example of this pH variability is shown for May 2015 (e).

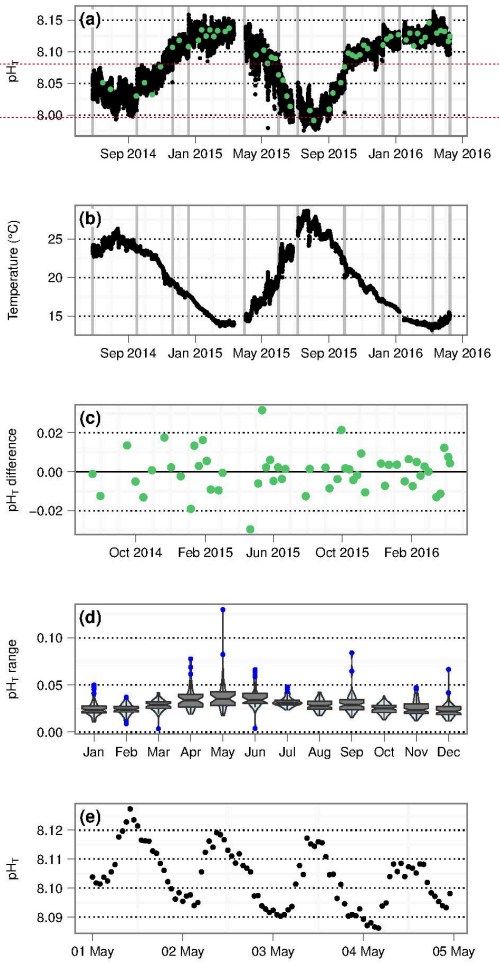


Deleted: autonomous

Deleted: buoy